Published in final edited form as:
Neuron. 2014 July 16; 83(2): 324–330. doi:10.1016/j.neuron.2014.06.008.

Control of interneuron firing by subthreshold synaptic potentials in principal cells of the dorsal cochlear nucleus

Pierre F. Apostolides[1,2,*] and **Laurence O. Trussell**[2]

[1]Neuroscience Graduate Program, Oregon Health & Science University. Portland, Oregon, 97239, USA

[2]Vollum Institute & Oregon Hearing Research Center, Oregon Health & Science University. Portland, Oregon, 97239, USA

Abstract

Voltage-gated ion channels amplify, compartmentalize, and normalize synaptic signals received by neurons. We show that voltage-gated channels activated during subthreshold glutamatergic synaptic potentials in a principal cell generate an excitatory→inhibitory synaptic sequence that excites electrically-coupled interneurons. In fusiform cells of the dorsal cochlear nucleus, excitatory synapses activate a TTX-sensitive Na^+ conductance and deactivate a resting I_h conductance, leading to a striking reshaping of the synaptic potential. Subthreshold voltage changes resulting from activation/deactivation of these channels subsequently propagate through gap junctions, causing slow excitation followed by inhibition in GABAergic stellate interneurons. Gap junction-mediated transmission of voltage-gated signals accounts for the majority of glutamatergic signaling to interneurons, such that subthreshold synaptic events from a single principal cell are sufficient to drive spikes in coupled interneurons. Thus, the interaction between a principal cell's synaptic and voltage-gated channels may determine the spike activity of networks without firing a single action potential.

Introduction

Inhibitory interneurons sharpen the temporal integration of excitatory inputs and control spikes in principal cells during afferent activity, thereby tempering network excitation and enhancing the signal-to-noise of information relayed to downstream brain regions (Cruikshank et al., 2007; Santamaria et al., 2007; Isaacson and Scanziani, 2011; Haider et al., 2013). Interestingly, interneurons in many brain regions are electrically-coupled via gap

Correspondence: Laurence O. Trussell, 3181 SW Sam Jackson Park Rd, L335A, Portland OR 97221, Phone 503-494-3424, trussell@ohsu.edu.
*Present address: Janelia Farm Research Campus / HHMI, 19700 Helix Dr, Ashburn, VA 20147

Author contributions:
P.F.A. performed the experiments. P.F.A. and L.O.T. designed the study, analyzed and interpreted the results, and wrote the paper.

junctions, allowing multiple interneurons to synchronize their spiking (Mann-Metzer and Yarom, 1999; Dugué et al., 2009). Although gap junctions act as low-pass filters and preferentially transmit slow voltage signals such as subthreshold synaptic events rather than fast, supra-threshold spikes (Bennett and Zukin, 2004), many previous studies investigating gap junctions focused primarily on transmission of action potentials (Mann-Metzer and Yarom, 1999; Christie et al., 2005; Dugué et al., 2009; Apostolides and Trussell, 2013; but see Zsiros et al., 2007; Lamotte d'Incamps and Ascher, 2012). How subthreshold depolarizations propagate through electrical networks, and whether they represent a physiologically relevant signal is unclear.

In the cerebellum-like dorsal cochlear nucleus (DCN), granule cell parallel fibers relaying sensory information form sparse excitatory synapses with projection neurons (fusiform cells) and inhibitory molecular layer interneurons. This organization implies that neighboring cells are activated by different sets of parallel fibers, and that local inhibition is not recruited in a traditional “feedforward” manner (Roberts and Trussell, 2010). However, fusiform cells are electrically coupled to small, high-impedance GABAergic interneurons (stellate cells; Apostolides and Trussell, 2013, 2014). Do subthreshold synaptic inputs in fusiform cells excite stellate cells? If so, this would allow the lateral activation of stellate cells across divergent parallel fibers, ensuring recruitment of local inhibition despite sparse convergence from excitatory synapses. Using patch-clamp recordings in acute slices of mouse DCN, we show that parallel fiber synapses onto fusiform cells activate a long-lasting Na^+ conductance at subthreshold voltages and deactivate a hyperpolarization-activated cyclic-nucleotide gated (HCN or I_H) conductance. Transmission of this synaptic and voltage-gated waveform through electrical synapses profoundly alters the time course and amplitude of excitatory transmission onto stellate cells and drives spikes in an inhibitory network.

Results

Glutamate release generates a non-canonical excitatory→inhibitory (E/I) sequence in stellate cells

Stellate and fusiform cells receive excitatory synapses from parallel fibers in the DCN molecular layer (Figure 1A; Wouterlood et al., 1984). In stellate cells voltage-clamped at -67 mV, single shocks to parallel fibers (see Supplemental Methods) caused a multiphasic response with an early inward and a late outward component (Figure 1B). The outward component was not due to glycine or $GABA_A$ receptors, as all experiments were performed in the presence of strychnine (1–2 μM) and SR95531 (10 μM). Interestingly, NBQX (10 μM) abolished both inward and outward components (n=7), indicating that AMPA receptor activation triggered excitatory and inhibitory responses (Figure 1B, red trace).

Close inspection of the traces revealed trial-to-trial variation in the responses to parallel fiber stimulation. Some events had an initial rapidly rising and decaying inward component that resembled a fast AMPA receptor-mediated excitatory postsynaptic current (EPSC) and were followed by the slow inward and outward phases. Other events lacked the initial fast phase, yet maintained identical slow inward and outward components (n=11; Figure 1B, right, black and gray traces, respectively). This slow component accounted for 75±7% of the total

inward charge transfer. The stimulus intensity was adjusted to evoke initial fast-rising currents in approximately half of the trials; we thus interpret the variable appearance of the fast inward component as reflecting quantal fluctuation of release from single parallel fiber synapses on the recorded stellate cells. Given that AMPA receptors in DCN stellate cells display rapid rise and decay kinetics (Apostolides and Trussell, 2014), the drastically slower kinetics and comparatively invariant nature of the later components shown in Figure 1B suggest that these "synaptic" currents originate in fusiform cells electrically-coupled to the voltage-clamped stellate cell.

Accordingly, stellate cell EPSCs recorded in slices from mutant mice lacking electrical coupling in the DCN (connexin36−/− mice; cx36−/−) fluctuated between a purely fast inward current or no current at all (n=12 cells; Figure 1C). The slow outward component was also absent in cx36−/− mice, indicating that it similarly originated from prejunctional fusiform cells. The total inward charge transfer of EPSCs from cx36−/− mice was much smaller than EPSCs of WT mice, suggesting that parallel fiber inputs passing through fusiform cells represent the majority of synaptic excitation for stellate cells in WT mice under these stimulus conditions (Figure 1D, left panel). However, the charge and peak amplitude of the fast AMPA component (representing parallel fiber transmission directly onto the voltage-clamped stellate cell) was similar across genotypes, arguing that these differences were not due to general deficits in parallel fiber transmission in mutant mice (Figure 1D, middle and right panels). In summary, our data show that the majority of excitation in stellate cells is inherited from prejunctional fusiform cells during sparse parallel fiber activity.

A Na^+ conductance determines the kinetics and gain of EPSPs in fusiform cells

Excitatory synapses can activate Ca^{2+} and Na^+ channels that shape excitatory postsynaptic potentials (EPSPs; Stuart and Sakmann, 1995; Higler and Sabatini, 2010; Carter et al., 2012). Given that fusiform cells express a long-lasting Na^+ current that is active at subthreshold voltages (Leao et al., 2012), we hypothesized that subthreshold excitation might activate this current and broaden parallel fiber-fusiform cell EPSPs. If so, the slow inward component observed in stellate cells (Figure 1B) would not merely represent a passive depolarization of fusiform cell dendrites during EPSPs, but rather an active subthreshold depolarization by Na^+ currents in prejunctional fusiform cells.

We tested whether subthreshold EPSPs activate Na^+ channels in fusiform cells by injecting EPSC-like waveforms through the patch pipette and quantifying the effect of the Na^+ channel blocker tetrodotoxin (TTX, 1 μM) on the resulting artificial EPSPs (aEPSPs). Increasing the EPSC waveform amplitude generated progressively larger aEPSPs whose half-widths were markedly dependent on the EPSC waveform amplitude: aEPSPs evoked with 100–200 pA waveforms had significantly smaller half-widths than aEPSPs evoked with 250–700 pA waveforms (Figure 2A,B; 44±8 vs 77±14 ms, p=0.003, paired t-test). TTX abolished this amplitude-dependence of aEPSP half-width, and linear fits to the aEPSP peak amplitude values further revealed that Na^+ channels control the slope of the excitatory input/output curve (Figure 2B, right panel). The amplitude range of EPSC waveforms in these experiments is similar to that of sound-evoked EPSCs recorded from fusiform cells *in vivo*

(Zhou et al., 2012). Furthermore, previous data show that parallel fiber EPSCs <500 pA (corresponding to ~10 simultaneously active parallel fibers) drive spiking in less than 50% of trials (Roberts and Trussell, 2010). Since the mean amplitude of the largest EPSC waveform we used to trigger the Na^+ conductance at subthreshold potentials was 471±58 pA, (n=7), these findings suggest that the majority of naturally occurring parallel fiber activity on fusiform cells which does not drive action potentials would be expected to activate the TTX-sensitive Na^+ conductance.

Interestingly, an afterhyperpolarization (AHP) often followed the aEPSPs (Figure 2A, asterisk), suggesting that the outward current observed in stellate cells (Figure 1) might also result from subthreshold events in fusiform cells. TTX reduced this AHP to 39±8% of baseline (n=7 cells), which was likely secondary to an effect of TTX on aEPSP half-width: In 3 cells tested in TTX, increasing the decay time constant of the EPSC waveform from 3 to 10 ms rescued the original AHP amplitude (baseline amplitude with 3 ms decay: −1.4±0.3 mV, in TTX with 3-ms decay: −0.8±0.2 mV, in TTX with 10-ms decay: −1.6±0.3 mV). Altogether, these data show that Na^+ currents activated by subthreshold depolarizations control the size and duration of excitatory signals, and predict that Na^+ channels located on prejunctional fusiform cells play a major role in shaping transmission in electrically-coupled stellate cells.

Subthreshold activation of voltage-gated Na^+ channels in fusiform cells generates slow excitation in stellate cells

Given that Na^+ channels have such a profound effect on aEPSPs, we tested whether subthreshold events in fusiform cells transmit a TTX-sensitive current to stellate cells by recording from electrically-coupled fusiform-stellate cell pairs and driving aEPSPs in the fusiform cell while voltage-clamping the stellate cell (Figure 2C). The aEPSPs generated time-locked postjunctional inward currents in stellate cells, showing that subthreshold events in fusiform cells are reliably transmitted through gap junctions (n=6 pairs. Figure 2C, black trace). TTX significantly reduced the peak amplitude and half-width of aEPSPs in fusiform cells (to 73±3% and 32±5% of baseline, respectively), mirrored by a prominent reduction in peak amplitude and charge transfer of the postjunctional currents in the stellate cell (Figure 2C,D). This effect was not due to secondary activation of Na^+ channels on stellate cells, as Na^+ channels were pre-blocked in all experiments by the addition of QX314 (5 mM) specifically to the stellate cell internal solution. Thus, subthreshold activation of voltage-gated Na^+ channels in single neurons shapes excitatory transmission in a network of neurons.

AHPs following sub- and suprathreshold responses in fusiform cells are mediated by deactivation of I_h

The AHP following aEPSPs (Figure 2A) might represent a synaptic “off-response” that could generate the slow outward current (Figure 1B) and provide long-lasting inhibition to stellate cells following excitatory signals. Interestingly, the half-width of the subthreshold AHPs following aEPSPs (352±24 ms, n=19 cells) resembled that of the fusiform cell post-spike burst AHP reported in a previous study (406±58 ms; Apostolides and Trussell, 2013). Furthermore, the slow outward current recorded in stellate cells (Figure 1B) also resembled

the current mediated by gap junction propagation of the fusiform cell post-spike burst (Apostolides and Trussell, 2013). Thus, the same biophysical mechanism might underlie AHPs generated by sub- or suprathreshold activity in fusiform cells, and the resulting voltage deflection would generate a net outward current in stellate cells.

Given a recent study showing that HCN channels control the resting membrane potential of fusiform cells (Rusznák et al., 2013), we hypothesized that HCN channels could mediate the AHP: Because HCN channels activate upon hyperpolarization and deactivate during depolarization, action potentials or subthreshold EPSPs will deactivate the HCN channels that are open at rest, thereby transiently bringing the membrane potential below rest after an excitatory event. The decay kinetics of the AHP would therefore follow the re-activation kinetics of HCN channels. We first evaluated the effect of the HCN channel blocker CsCl (3 mM) on the AHP following aEPSPs in fusiform cells. CsCl hyperpolarized fusiform cells (n=7 cells. Baseline: −70.3±1.4 mV. CsCl: −76±3.4 mV), in agreement with Rusznák et al. (2013). Surprisingly, CsCl also caused a concomitant *decrease* in the fusiform cell's input resistance, which was largely reversed by returning the membrane potential near its baseline level with bias current (baseline: 93.2±10.8 MOhm, CsCl: 57.2±6.8 MOhm, CsCl + bias current: 88.3±13 MOhm. p=0.002, one-way repeated measures ANOVA + Bonferroni test comparing baseline and CsCl; n.s. comparing baseline and CsCl + bias current. Membrane potential in CsCl + bias current condition: −70.0±1.4 mV). The voltage-dependent drop in membrane resistance is likely due to activation of inward rectifier K^+ conductance, as described previously (Leao et al., 2012). In agreement with a HCN-mediated mechanism, CsCl blocked the AHP following aEPSPs (n=7, Figure 3A+inset). Returning the membrane potential back to its original value did not recover the AHP, indicating that this was not due to a shunting effect.

HCN current promotes the activation of the Na^+ conductance

Blocking HCN channels is expected to hyperpolarize fusiform cells away from the activation range for Na^+ currents that shape subthreshold events (e.g., Figure 2), thereby altering the timecourse of aEPSPs. Indeed, CsCl reduced the amplitude and half-width of aEPSPs, and this effect was largely reversed by returning the membrane potential to near baseline values (n=7, Figure 3A). The unusual voltage-dependence of aEPSP half-widths highlights a novel role for HCN channels in temporal integration by setting the resting membrane potential near the activation range for a Na^+ current. Thus, HCN channels in fusiform cells might shape excitation in stellate cells in two ways: Basal HCN activity would determine the half-width of slow inward currents in stellate cells by controlling whether parallel fibers onto fusiform cells activate the Na^+ conductance, whereas transient deactivation of HCN channels following fusiform cell EPSPs would cause a slow hyperpolarization. Thus, blocking HCN channels should reduce the half-width of inward currents and block the outward currents following parallel fiber stimuli in voltage-clamped stellate cells. Accordingly, CsCl reduced the inward charge transfer of EPSCs and blocked the subsequent outward current in stellate cells (Figure 3B, n=8), and similar reductions were observed with another HCN channel blocker (ZD7288, 20 μM. n=4, data not shown). Thus, the interplay between subthreshold activation of Na^+ currents, I_h, and gap junctions

generates a synaptic E/I sequence in local interneurons that persists for several hundred milliseconds.

Spike-driven AHPs are partially mediated by HCN channels

Is parallel fiber activity required for HCN-mediated inhibition in stellate cells, or does depolarizing the prejunctional fusiform cells suffice? We distinguished between these two possibilities by testing whether AHPs following spike trains in fusiform cells generate CsCl-sensitive outward currents in stellate cells. Square pulse current injections in fusiform cells drove spike trains followed by a prominent AHP (Figure 3C; see also Apostolides and Trussell, 2013). Bath application of CsCl hyperpolarized fusiform cells, as previously mentioned. We injected positive bias current in CsCl to maintain the cell's membrane potential near the baseline value (n=6. pre-CsCl: −73.1±1.8 mV; post CsCl: −73.5±1.0 mV. p=0.63, paired t-test), but the AHP was still reduced to 53±5% of baseline (Figure 3C, n=6). Thus, HCN channels mediate approximately half of the spike train-triggered AHP in fusiform cells. In mice expressing channelrhodopsin2 specifically in fusiform cells (see Methods), light stimuli generate biphasic postjunctional photocurrents in voltage-clamped stellate cells that are due to spike trains in prejunctional fusiform cells (Apostolides and Trussell, 2013). These photocurrents are characterized by a steady state inward component followed by a slow outward component upon light termination. Similar to results with parallel fiber stimuli (Figure 3B), the outward component was strongly reduced by CsCl (n=7, Figure 3D), thus confirming that depolarizing fusiform cells is sufficient to generate HCN-mediated inhibition in stellate cells.

Subthreshold events in fusiform cells drive stellate cell spiking

The lowpass filter properties of gap junctions predict that slow events such as EPSPs might be significantly more potent than spikes in regulating the membrane potential of postjunctional cells. Do synaptic events that fail to generate action potentials in fusiform cells nevertheless bring the stellate cell membrane potential above spike threshold? We tested this idea by recording from electrically-coupled pairs, evoking aEPSPs in prejunctional fusiform cells, and quantifying the number of spikes per 50-ms bin in postjunctional stellate cells. Fusiform cell aEPSPs caused time-locked spikes in stellate cells in a number of trials (n=7 pairs, Figures 4A–D). In some pairs, the stellate cell's spontaneous firing rate was reduced during the ~200–400 ms following the aEPSP, corresponding to the timing of the fusiform cell subthreshold AHP. However, this reduction was not statistically significant in grouped data (one-way repeated measures ANOVA + Dunnett's test), suggesting that a significant reduction in stellate cell spike rate may require summation of subthreshold events from multiple prejunctional fusiform cells. Thus, subthreshold excitatory events in a single principal neuron can drive spikes in its electrically-coupled neighbors, thereby increasing the range of presynaptic parallel fibers which recruit inhibitory interneurons.

Discussion

We have shown that in addition to canonical mechanisms of synaptic transmission, the strength and kinetics of excitatory transmission onto DCN stellate cells are controlled by

synapses located on prejunctional fusiform cells. Specifically, parallel fiber synapses trigger an E/I sequence mediated by the spread of voltage-gated events through gap junctions.

Although stellate cells express fast-gating, Ca^{2+}-permeable AMPA receptors (Apostolides and Trussell, 2014), the time course of EPSCs can be surprisingly slow (Figure 1). We find that a Na^{+} current activated by subthreshold EPSPs in fusiform cells accounts for this paradox. Furthermore, a hyperpolarization following deactivation of the resting HCN conductance in fusiform cells caused a net outward current in stellate cells, highlighting a novel biophysical mechanism by which excitatory synapses generate complex synaptic E/I sequences. More generally, our data reveal a functional architecture that dramatically increases a neuron's total number of presynaptic inputs in a manner not expected from the established anatomical circuit. Thus, these data reveal an anatomical and biophysical setting in which subthreshold activity in prejunctional neurons drives the suprathreshold activity of postjunctional neurons.

Electrical coupling, HCN channels, and subthreshold activation of TTX-sensitive Na^{+} channels are all common features of neurons found in diverse brain regions (Christie et al., 1989; Curti and Pereda, 2004; Christie et al., 2005; Haas and Landisman, 2012; Lamotte d'Incamps and Ascher, 2012). Together with our study, these findings imply that the interplay between activation of voltage-gated channels on single cells and network-wide gap junction coupling may shape synaptic transmission in diverse neuronal microcircuits.

Methods

See online Supplemental Methods.

Supplementary Material

Refer to Web version on PubMed Central for supplementary material.

Acknowledgments

We thank Michael Bateschell and Ruby Larisch for help with mouse colony management, and Delia Chiu, Brett Carter, and members of the Trussell Lab for helpful discussions during the course of these experiments. Funding was provided by NIH grants R01DC004450 and R01NS28901 (L.O.T.) and 1F31DC012222 (P.F.A.)

References

Apostolides PF, Trussell LO. Regulation of interneuron excitability by gap junction coupling with principal cells. Nat Neurosci. 2013; 16:1764–1772. [PubMed: 24185427]

Apostolides PF, Trussell LO. Chemical synaptic transmission onto superficial stellate cells of the dorsal cochlear nucleus. J Neurophysiol. 2014

Bennett MVL, Zukin RS. Electrical coupling and neuronal synchronization in the Mammalian brain. Neuron. 2004; 41:495–511. [PubMed: 14980200]

Carter BC, Giessel AJ, Sabatini BL, Bean BP. Transient sodium current at subthreshold voltages: activation by EPSP waveforms. Neuron. 2012; 75:1081–1093. [PubMed: 22998875]

Christie JM, Bark C, Hormuzdi SG, Helbig I, Monyer H, Westbrook GL. Connexin36 mediates spike synchrony in olfactory bulb glomeruli. Neuron. 2005; 46:761–772. [PubMed: 15924862]

Christie MJ, Williams JT, North RA. Electrical coupling synchronizes subthreshold activity in locus coeruleus neurons in vitro from neonatal rats. J Neurosci. 1989; 9:3584–3589. [PubMed: 2795142]

Cruikshank SJ, Lewis TJ, Connors BW. Synaptic basis for intense thalamocortical activation of feedforward inhibitory cells in neocortex. Nat Neurosci. 2007; 10:462–468. [PubMed: 17334362]

Dugué GP, Brunel N, Hakim V, Schwartz E, Chat M, Lévesque M, Courtemanche R, Léna C, Dieudonné S. Electrical coupling mediates tunable low-frequency oscillations and resonance in the cerebellar Golgi cell network. Neuron. 2009; 61:126–139. [PubMed: 19146818]

Haider B, Häusser M, Carandini M. Inhibition dominates sensory responses in the awake cortex. Nature. 2013; 493:97–100. [PubMed: 23172139]

Haas JS, Landisman CE. State-dependent modulation of gap junction signaling by the persistent sodium current. Front Cell Neurosci. 2012; 5:3.

Isaacson JS, Scanziani M. How inhibition shapes cortical activity. Neuron. 2011; 72:231–243. [PubMed: 22017986]

Lamotte-d'Incamps B, Ascher P. Four Excitatory Postsynaptic ionotropic receptors coactivated at the motoneuron–Renshaw cell synapse. J Neurosci. 2008; 28:14121–14131. [PubMed: 19109494]

Leao RM, Li S, Doiron B, Tzounopoulos T. Diverse levels of an inwardly rectifying potassium conductance generate heterogeneous neuronal behavior in a population of dorsal cochlear nucleus pyramidal neurons. J Neurophysiol. 2012; 107:3008–3019. [PubMed: 22378165]

Mann-Metzer P, Yarom Y. Electrotonic coupling interacts with intrinsic properties to generate synchronized activity in cerebellar networks of inhibitory interneurons. J Neurosci. 1999; 19:3298–3306. [PubMed: 10212289]

Parri HR, Crunelli V. Sodium current in rat and cat thalamocortical neurons: role of a non-inactivating component in tonic and burst firing. J Neurosci. 1998; 18:854–867. [PubMed: 9437007]

Roberts MT, Trussell LO. Molecular layer inhibitory interneurons provide feedforward and lateral inhibition in the dorsal cochlear nucleus. J Neurophysiol. 2010; 104:2462–2473. [PubMed: 20719922]

Rusznák Z, Pál B, Kőszeghy A, Fu Y, Szücs G, Paxinos G. The hyperpolarization-activated non-specific cation current (In) adjusts the membrane properties, excitability, and activity pattern of the giant cells in the rat dorsal cochlear nucleus. Eur J Neurosci. 2013; 37:876–890. [PubMed: 23301797]

Santamaria F, Tripp PG, Bower JM. Feedforward inhibition controls the spread of granule cell-induced Purkinje cell activity in the cerebellar cortex. J Neurophysiol. 2007; 97:248–263. [PubMed: 17050824]

Stuart G, Sakmann B. Amplification of EPSPs by axosomatic sodium channels in neocortical pyramidal neurons. Neuron. 1995; 15:1065–1076. [PubMed: 7576650]

Wouterlood FG, Mugnaini E, Osen KK, Dahl AL. Stellate neurons in rat dorsal cochlear nucleus studies with combined Golgi impregnation and electron microscopy: synaptic connections and mutual coupling by gap junctions. J Neurocytol. 1984; 13:639–664. [PubMed: 6481413]

Zhou M, Tao HW, Zhang LI. Generation of intensity selectivity by differential synaptic tuning: fast-saturating excitation but slow-saturating inhibition. J Neurosci. 2012; 32:18068–78. [PubMed: 23238722]

Zsiros V, Aradi I, Maccaferri G. Propagation of postsynaptic currents and potentials via gap junctions in GABAergic networks of the rat hippocampus. J Physiol. 2007; 578:527–544. [PubMed: 17110410]

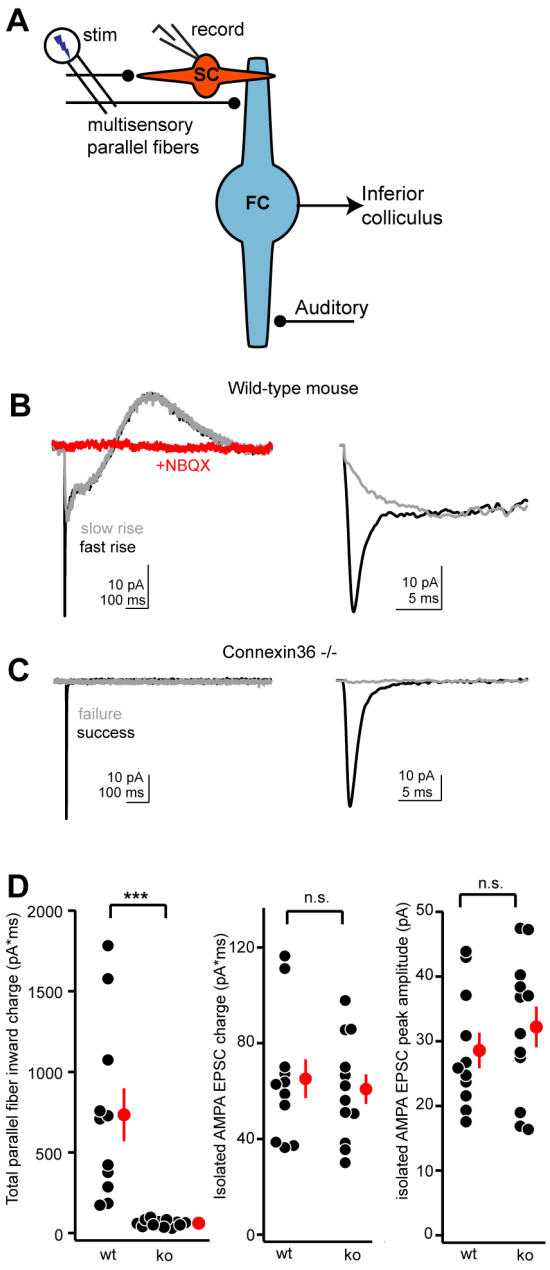

Figure 1.

Parallel fiber transmission generates an E/I sequence mediated by AMPA receptors.

A) DCN circuit and experimental set-up. Projection neurons (fusiform cells; FC) integrate excitatory synapses from auditory nerve and granule cell parallel fibers. The latter also contact the stellate interneurons that are electrically coupled to fusiform cells. A bipolar stimulating electrode is placed in the molecular layer to activate parallel fibers.

B) A single parallel fiber shock generates an E/I sequence in stellate cells that is blocked by the AMPA receptor antagonist NBQX (10 μM; red trace). Black trace is an average of events that had an initial rapidly rising component, whereas the gray trace is an average of

events lacking the fast component. The right panel shows the two types of events on a faster time base to highlight the drastic difference in rise times.

C) Parallel fiber EPSCs in cx36 −/− mice lack the slow inward and outward components. Black and gray traces represent averages of trials in which the fast component either succeeded or failed, respectively.

D) Quantification of EPSCs from wild-type and cx36 −/− mice. Left panel: The total inward charge transfer of parallel fiber EPSCs in wild-type mice was on average −734±164 pA*ms (n=11), whereas it was only −62±6 pA*ms in the KO mice (n=12). Middle and right panels: The inward charge transfer and peak amplitude of the fast rising AMPA EPSC from parallel fiber synapses directly on stellate cells was not significantly different between wild-type and KO mice (WT charge and peak amplitude: −65±8 pA*ms, −29±3 pA. KO charge and peak amplitude: −60±6 pA*ms, −32±3 pA. p=0.67 and 0.39, respectively; unpaired t-test). The fast rising AMPA EPSC was isolated by subtracting the average of slowly-rising events from the average of fast rising events (e.g., black trace minus gray trace).

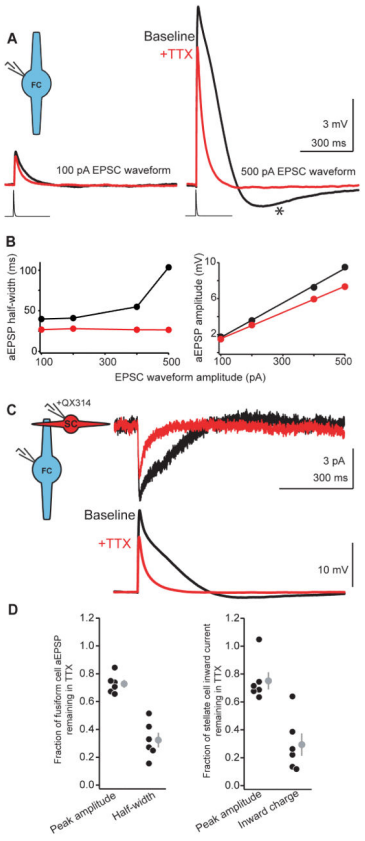

Figure 2.

Subthreshold activation of Na^+ channels in fusiform cells shapes excitatory transmission in electrically-coupled stellate cells.

A) Example traces from a fusiform cell in current-clamp. An EPSC waveform is injected at two different amplitudes (100 and 500 pA) before and after bath application of TTX (black and red traces, respectively). The differential kinetics of the black traces highlights the role of Na^+ channels in shaping the aEPSP half-width. TTX application reduced the aEPSP half-width and peak amplitude, showing that subthreshold depolarizations activate Na^+ channels. Note the AHP following the aEPSP evoked with a 500 pA waveform. Resting voltages for 100 pA events: −70 mV (control), −71 mV (TTX); for 500 pA events: −72 mV (control), −71 mV (TTX).

B) Example input/output curves for the example cell shown in panel (A). Left panel: aEPSP half-widths as a function of EPSC waveform amplitude before and after TTX (black and red points, respectively). In n=7 cells, aEPSP half-widths evoked with the largest EPSC waveform amplitude (mean: 471±58 pA, range: 250–700 pA) were on average 2.4±0.4 times greater than aEPSP half-widths evoked with the smallest amplitude waveform (mean: 114±24 pA, range: 50–200 pA). This ratio was reduced to 1.0±0.1 in TTX (p=0.007, paired t-test), showing that Na^+ channels powerfully control the kinetics of subthreshold events. Right panel: aEPSP peak amplitudes plotted as a function of EPSC command waveform in baseline and after TTX. Color scheme is the same as left panel. The dotted lines are linear fits to the data points to calculate the slope of the input/output function. On average, TTX

reduced the slope of the aEPSP amplitude function to 77±3% of baseline (0.027±0.004 mV/pA in baseline to 0.020±0.003 mV/pA in TTX, n=7 cells, p=0.007, paired t-test).

C) Left: diagram of paired recording experiment. Na^+ channels are blocked specifically in the stellate cell by the addition of the Na^+ channel blocker QX314 to the stellate cell pipette internal solution. Right: Average traces showing a subthreshold aEPSP in a fusiform cell (lower panel) and the resulting inward current in the stellate cell (upper panel) before and after TTX (black and red traces, respectively). TTX reduced the amplitude and half-width of aEPSPs in the fusiform cell. TTX similarly reduced the amplitude and charge transfer of the postjunctional inward current in the stellate cell, showing that Na^+ channels in fusiform cells are a significant source of excitation. Resting voltages for fusiform cell pre-TTX, −75 mV; post-TTX: −74 mV.

D) Summary data from 6 pairs similar to C. Left: TTX reduced the amplitude and half-width of fusiform cell aEPSPs to 73±3% and 32±5% of baseline (p=0.0002 and p<0.0001, respectively, one sample t-test). Right: TTX also significantly reduced the amplitude and inward charge transfer of postjunctional currents in stellate cells to 75±6% and 29±8% of baseline (p=0.0097 and p=0.0003, respectively, one sample t-test). Gray points are mean ±SEM.

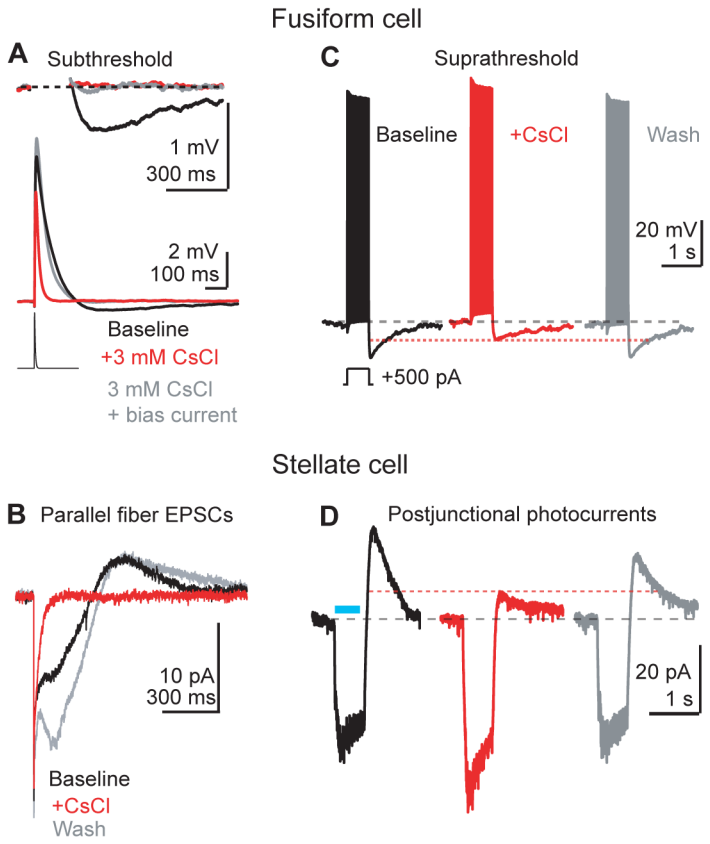

Figure 3.

Fusiform cell AHPs and stellate cell off-responses are mediated by deactivation of HCN channels.

A) An EPSC waveform (500 pA, lower trace) is injected in a fusiform cell in current clamp. CsCl (red trace) hyperpolarized the cell (see main text), and significantly shortened the half-width and reduced the peak amplitude of aEPSPs. These effects were largely reversed by returning the membrane potential to near baseline values with positive current (gray trace), showing that HCN channels control EPSP kinetics by setting the resting membrane potential near the activation range for subthreshold Na^+ currents (n=7 cells. Peak amplitude baseline: 7.8±0.6 mV; CsCl 6.0±0.5 mV; CsCl + bias current: 8.8±0.6 mV. p=0.0007 and p=0.13 comparing baseline to CsCl and CsCl + Bias conditions, respectively. Repeated measures ANOVA + Dunnett's test. Half-width baseline: 47±6 ms; CsCl: 15±1 ms; CsCl + bias: 36±3 ms; p=0.002 and p=0.076 comparing baseline to CsCl and CsCl+Bias, respectively. Repeated measures ANOVA + Dunnett's test). Blocking HCN channels reduced the AHP following the depolarizing phase of the aEPSP, but adding bias current in the presence of CsCl failed to recover the AHP following the aEPSP (baseline: −0.39±0.08 mV; CsCl: −0.05 ±0.02 mV; CsCl + Bias current −0.03±0.01 mV, p= 0.014 and p=0.001 comparing baseline to CsCl and CsCl + Bias, respectively. Repeated measures ANOVA + Dunnett's test). Resting voltage of fusiform cell pre CsCl, −69 mV; in CsCl, −75 mV; in CsCl + bias current, −71 mV.

B) A stellate cell is recorded in voltage clamp. Parallel fibers are stimulated with a single shock, generating the biphasic E/I sequence shown in Figure 1B. CsCl significantly reduced the slow outward current to 1±2% of baseline (n=8. $p<0.0001$, one-sample t-test). Additionally CsCl hastened the timecourse of the inward component, quantified as a reduction of the EPSC inward charge transfer (n=8. 26±3% of baseline remaining, $p=0.01$, one sample t-test).

C) A fusiform cell is driven to spike with positive current injection. CsCl (3 mM, middle red panel) significantly reduced the amplitude of the AHP to 54±5% of baseline (n=6. $p=0.0002$, one sample t-test). Resting voltage of fusiform cell control, −78 mV; in CsCl: −78 mV; wash, −78 mV. Single sweeps are shown.

D) Example from a voltage-clamped stellate cell in a VGluT2-ChR2 mouse. Prejunctional fusiform cells are activated with blue light flashes through the microscope objective (blue bar), generating a biphasic postjunctional response. The outward component, which represents the fusiform cell membrane potential returning towards baseline during the AHP, was reversibly reduced by CsCl to 40±12% of baseline (n=7, $p<0.0001$. One sample t-test).

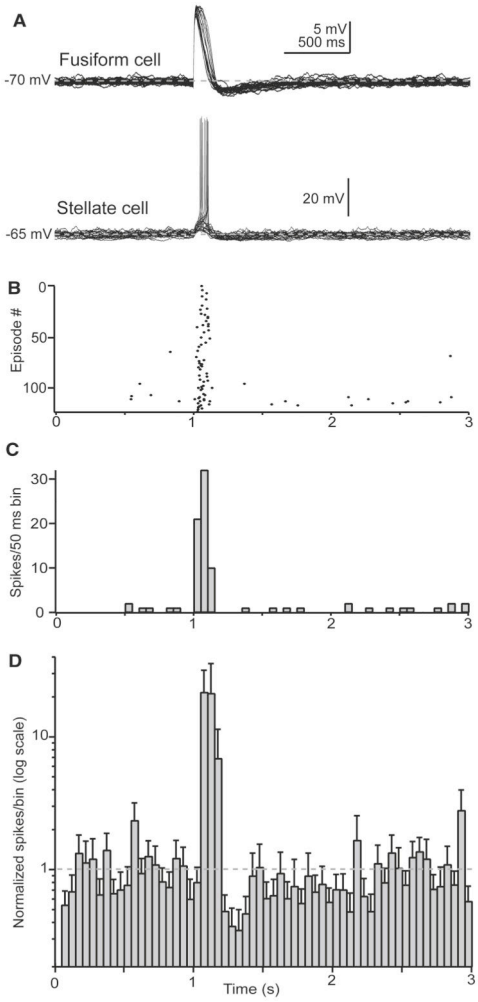

Figure 4.

Subthreshold events in fusiform cells drive spikes in stellate cells.

A) Example recording (20 single trials) from a coupled fusiform-stellate cell pair (upper and lower panels, respectively). A subthreshold aEPSP is produced by injecting an EPSC-like waveform into the fusiform cell at ΔT=1 s (peak amplitude: 350 pA). Of note is the clustering of spikes in the stellate cell recording specifically during the fusiform cell aEPSP.

B) Raster plot showing 123 trials from the pair in A. Subthreshold events in the fusiform cell cause time-locked spikes in the stellate cell.

C) Histogram (50 ms bins) from the same pair as panels A and B.

D) Summary histogram (50 ms bins) from 7 pairs as in A–C. The data are normalized to the number of spikes/bin during the 1 s prior to EPSC injection in the fusiform cell.

Subthreshold events in fusiform cells caused a 21±12 fold increase in the number of stellate cell spikes/bin at ΔT=1.05–1.1 s, followed by a non-significant reduction in spike count at ΔT=1.2–1.4 s (baseline: 7.4±3.9 spikes/bin; ΔT=1.05–1.1 s: 34.9±9.0 spikes/bin; ΔT=1.2–1.4 s: 6.1±4.4 spikes/bin, p=0.01 and 0.2 compared to baseline, respectively. Repeated

measures ANOVA + Dunnett's test). Of note is that the y-axis is plotted on a logarithmic scale.